IJC Metabolic & Endocrine 6 (2015) 17–23

Contents lists available at ScienceDirect

IJC Metabolic & Endocrine

journal homepage: http://www.journals.elsevier.com/ijc-metabolic-and-endocrine

Cardiac Metabolism in a Pig Model of Ischemia–Reperfusion by Cardiac Magnetic Resonance with Hyperpolarized 13C-Pyruvate

Giovanni Donato Aquaro [a,*], Francesca Frijia [a], Vincenzo Positano [a], Luca Menichetti [b], Maria Filomena Santarelli [b], Vincenzo Lionetti [c], Giulio Giovannetti [b], Fabio Anastasio Recchia [d], Luigi Landini [a]

[a] Fondazione G. Monasterio CNR-Regione Toscana, Pisa, Italy
[b] C.N.R. Institute of Clinical Physiology, Pisa, Italy
[c] Gruppo Intini-SMA Laboratory of Experimental Cardiology, Institute of Life Sciences, Scuola Superiore Sant'Anna, Pisa, Italy
[d] Department of Physiology, Temple University School of Medicine, Philadelphia, PA, USA

ARTICLE INFO

Article history:
Received 17 July 2014
Received in revised form 8 January 2015
Accepted 13 January 2015
Available online 19 January 2015

Keywords:
13C-pyruvate
Cardiac metabolism
Magnetic resonance
Ischemia/reperfusion

ABSTRACT

Background: Magnetic resonance (MRI) with hyperpolarized ^{13}C-pyruvate is a new technique for the assessment of myocardial metabolism.
Aims: The aim of this study is to assess the effectiveness of MRI with hyperpolarized ^{13}C-pyruvate to detect cardiac metabolic changes in a model of ischemia/reperfusion.
Methods: A pneumatic occluder was placed around the left anterior descending artery in 7 pigs. A 3 T scanner with a ^{13}C quadrature birdcage coil was used. Hyperpolarized ^{13}C-pyruvate was injected intravenously at rest, during coronary occlusion and 5 min after reperfusion. Metabolic images were acquired using a 3D-IDEAL spiral CSI during the injection of ^{13}C-pyruvate and 3D-parametric maps of ^{13}C-pyruvate, ^{13}C-lactate and ^{13}C-bicarbonate were generated. Metabolic Activity Mismatch (MAM) was defined as the relative change between a) resting state and coronary occlusion or b) resting and reperfusion in all the myocardial segments.
Results: During occlusion, a decrease in ^{13}C-lactate ($-21 \pm 26\%$ vs baseline $3 \pm 16\%$, $P < 0.0001$) and ^{13}C-bicarbonate ($-29 \pm 34\%$ vs $33 \pm 52\%$, $P < 0.0001$) was found in myocardial segments at risk, as compared with remote segments. In ischemic segments, the ^{13}C-lactate signal increased during reperfusion ($20 \pm 42\%$ vs $-7 \pm 22\%$, $P = 0.0007$), while ^{13}C-bicarbonate was persistently reduced ($-38 \pm 27\%$ vs $36 \pm 51\%$, $p < 0.0001$).
Conclusions: ^{13}C-pyruvate MRI is able to detect transient changes in regional metabolism in an in-vivo model of myocardial ischemia–reperfusion.

1. Background

Magnetic resonance (MRI) with hyperpolarized 13C-labeled tracers is an emerging imaging technique for the evaluation of coronary artery anatomy, quantification of myocardial perfusion and a direct assessment of myocardial viability [1]. In particular, MRI with hyperpolarized 13C-pyruvate has allowed, for the first time, to evaluate cardiac metabolism in real time and in vivo [2–4]. Relative changes of pyruvate and of its metabolites lactate, alanine and bicarbonate can be monitored under normal conditions, during either acute ischemia or reperfusion, following short- or long-lasting coronary occlusion [5]. Differently from PET where FDG is not metabolized by myocites, the main advantage of hyperpolarized 13C-pyruvate MRI is that the metabolic fate of 13C-pyruvate and its metabolites is directly assessed. A recent study using hyperpolarized 13C-pyruvate showed increased levels of 13C-lactate after 10 min of global ischemia in isolated hearts [6]. Golman et al. combined conventional MRI scan and H13C by a single short-axis slice of chemical shift images (CSI) in a pig model of ischemia–reperfusion, demonstrating decreased 13C-bicarbonate production in stunned viable myocardial segments, after 15-minute coronary occlusion, and decreased 13C-bicarbonate and 13C-alanine production after 45-minute occlusion [7]. Recently, Lau et al. proposed a three-dimensional multislice cardiac-gated spiral 13C imaging approach, permitting whole-heart coverage [8]. A novel fast three-dimensional acquisition (3D IDEAL, Iterative DEcomposition of water and fat with Echo Asymmetric and Least-squares estimation, spiral CSI pulse sequene) was then implemented in a rat model, allowing a higher spatial resolution, over the whole heart, of the spectral representation of single metabolites, separately acquired [9,10].

The objective of this study was to evaluate the capability and accuracy of MRI with hyperpolarized [1-13C]-pyruvate using the fast three-dimensional pulse sequence to detect the presence and the regional distribution of transient cardiac metabolic changes in a pig model of ischemia/reperfusion.

* Corresponding author at: Fondazione G. Monasterio CNR-Regione Toscana, Via G.Moruzzi, 1, 56124 Pisa, Italy. Tel.: +39 050 315 2818; fax: +39 050 315 2166.
E-mail address: aquaro@ftgm.it (G.D. Aquaro).

http://dx.doi.org/10.1016/j.ijcme.2015.01.007

The objective of this study was to evaluate the capability and the accuracy of MRI with hyperpolarized [1-13C]-pyruvate using a 3D-IDEAL Spiral CSI pulse sequence to detect the presence and the regional distribution of metabolic changes in a pig model of acute ischemia and ischemia/reperfusion.

2. Methods

2.1. Pig instrumentation

Seven male pigs (38 ± 3 kg), fasted overnight, were sedated with a cocktail of tiletamine hydrochloride and zolazepam hydrochloride (8 mg kg^{-1} i.m.) and premedicated with atropine sulfate (0.1 mg kg^{-1} i.m.). General anesthesia was subsequently induced with propofol (2–4 mg kg^{-1} i.v.) and maintained with 1–2% isoflurane in 50% air and 50% oxygen. Ventilation was adjusted based on arterial blood gas values. U sterile conditions and a 3 mm diameter pneumatic coronary occluder (Kent Scientific Corporation Torrington, Connecticut—USA) was placed around the left anterior descending coronary artery below the second diagonal branch through a direct thoracotomy at the fifth intercostal space. After this procedure, the pigs were allowed to fully recover for 10 days. Animal instrumentation and experimental protocol were approved by the Animal Care Committee of the Italian Ministry of Health and was in accordance with the Italian law (DL-116, Jan. 27, 1992), which is in compliance with the National Institutes of Health publication Guide for the Care and Use of Laboratory Animals.

2.2. MRI scanning

MRI was performed after post-surgical recovery. The pigs were sedated with continuous infusion of propofol (2–4 mg kg^{-1} h^{-1} i.v.) and studied in spontaneous respiration. They were placed in the MRI scanner laying on the right side. The hyperpolarized [1-13C]pyruvate dose (0.13 mmol/kg dissolved in 20 ml of buffer solution) was administered over 10 s by manual injection into the right ear vein. Injections were performed at rest, during 2 min of full coronary occlusion and after 5 min of reperfusion following 10 min of occlusion.

Coronary occlusion was performed by injecting 2 ml of saline solution in the pneumatic occluder. Arterial O_2 saturation, cardiac electric activity and blood pressure were continuously monitored during the experiment.

At the end of the MRI protocol the pigs were sacrificed by injecting 20 ml of KCl saturated solution after anesthesia induced by 20 ml propofol. In four animals, the chest was reopened, the coronary occluder was inflated, the ascending aorta was clamped and 10 ml of 1% methylene blue was injected into the coronary tree through the aortic wall, as previously described [11]. Then the heart was excised, and 10 mm thick slices were cut and photographed. A qualitative and quantitative assessment of the area at risk was performed and segments were classified as normal or at risk (Fig. 1).

2.3. Hyperpolarization and image acquisition

[1-13C]pyruvate polarization was performed using Dynamic Nuclear Polarization (*Hypersense*, Oxford Instruments, Oxford, UK) [11]. The injection solution contained 230 mM of sodium [1-13C]pyruvate, 100 mM TRIS buffer, 0.27 mM Na 2EDTA and 20 microM Gd^{3+}-complex (*Dotarem*—Guerbet—France). The temperature of solution was approximately 37 °C and the pH ≈ 7.6. In order to achieve the optimal timing to lead the pyruvate conversion on its metabolites, i.e. lactate, alanine and bicarbonate, MRI acquisition started 20 s after the end of the bolus injection [4].

Image acquisition was done in a 3-T GE Excite HDxt (GE Healthcare, Waukesha, WI, USA) clinical scanner, using a 13C quadrature birdcage coil (Rapid Biomedical, Würzburg, Germany) in low-pass version (radius, 18.2 cm; length, 36 cm; 12 legs). The image acquisition protocol included acquisition of anatomical reference images and CSI. Anatomical images were acquired with the scanner body coil and a 2D TOF FSPGR sequence, ECG triggered, was used with TR = 16.6 ms, TE 2.7 ms, FOV = 30 × 30 cm, matrix 288 × 192. Twenty axial slices were acquired with a slice thickness of 5 mm (no spacing) to cover the entire heart. Metabolic information covering the heart were obtained using a 3D IDEAL spiral CSI prescribed on the same region imaged by the reference anatomical sequence. The IDEAL spiral CSI is based on single-shot spiral image encoding and echo-time shifting between

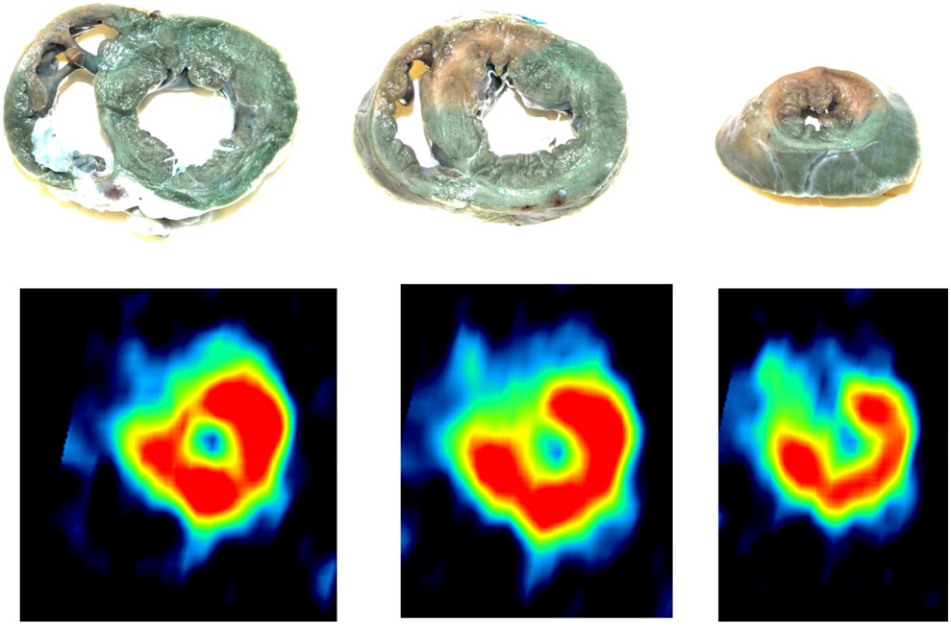

Fig. 1. Comparison between the histological analysis with methylene-blue (upper panels) and 13C-lactate reconstructed images (lower panels). In the sections of excised heart methylene-blue colorless segments corresponding to middle and apical anterior and anteroseptal myocardial segments represent the area at risk and matched with the region with absence of signal in the 13C-lactate reconstructed images.

excitations for the CSI encoding. 3D IDEAL spiral sequence was implemented in axial plane (FOV = 30 × 30 cm^2, slab thickness = 100 mm, 11 constant echo time shift of TE = 0.9 ms, FA = 7°, 14 phase encoding steps along the z-direction) with a resolution of 15 mm. The acquisition time for the 3D-IDEAL spiral was of 17 s and the sequence started 20 s after the beginning of the injection [4]. In addition, an FID spectrum is also acquired, and the obtained CSI prior knowledge is effectively utilized in the reconstruction, where it allows mapping of the full spectrum rather than a limited number of peaks at certain prescribed frequencies [12].

The data were reconstructed using spectrally-preconditioned, minimum-norm CSI inversion followed by gridding reconstruction implemented in Matlab (The Mathworks, Inc., Natick, MA).

2.4. Image analysis

Short axis (SA) views of left ventricle (LV) were reconstructed from axial anatomical images by using Gate tool of PMOD software (PMOD Technologies Ltd., Zurich, Switzerland). Briefly, the geometrical transformation used to extract SA views was recorded and applied to metabolic images that were reconstructed with the same orientation and resolution of anatomical SA images. Hence, 20 SA slices were involved in the image analysis process. Both anatomical and metabolic SA views were stored in DICOM format. Fig. 2 shows a typical example of corresponding anatomical and metabolic SA views extracted as previously described.

Quantitative analysis was performed on SA views by a custom software tool (HIPPO C13) developed in IDL 8.0 (Exelis Visual Information Solutions, Boulder, CO, USA). Myocardial contours were manually defined in anatomical SA views covering the entire LV (Fig. 2). A reference point corresponding to superior insertion of right and left ventricle wall was also defined. Slices were classified as basal, middle, or apical by the operator. Starting from the reference point, myocardium was divided in 120 micro sectors, and the metabolite signal in each micro sector was evaluated. Finally, a polar map was constructed by reporting the signal value in a "bull's eye" representation (Fig. 3). The polar map values were averaged among six (basal and medium slices) or four (apical slices) equiangular segments, and the values of metabolites concentration in corresponding segment of basal, middle, and apical slices were averaged as well leading to a 16-segments model of metabolite distribution, following the AHA guidelines [13].

To semi-quantitatively analyze the segmental distribution of metabolites signal over the LV wall, the segmental variation map was defined as $\Delta S_i = 100 \times (S_i - S_g) / Sg$, where S_i (i = 1,…16) is the relative metabolite signal in the segment *i* and S_g is the mean relative metabolite signal over the entire LV. To assess the differences among different conditions (i.e. basal, occlusion, reperfusion), the Metabolic Activity Mismatch (MAM) between two segmental variation maps was defined as $MAM = 100(S_{ai} - S_{bi}) / (S_{ai} + S_{bi}) / 2$, where S_{ai} and S_{bi} are the relative values of the signal of metabolite in the segment "i" in condition "a" and "b".

2.5. Hemodynamic study

Five additional male pigs (38 ± 3 kg) were chronically instrumented as previously described [14]. Briefly, a Doppler flow transducer (Craig Hartley) was placed around the left anterior descending coronary artery distally to the flow probe; the pneumatic vascular occluder was placed below the second diagonal branch of the LAD. Coronary blood flow was measured with a pulsed Doppler flowmeter (Model 100, Triton Technology). Arterial pressure was measured via a fluid filled catheter, while LV pressure, dP/dtmax and dP/dtmin were measured using a solid state pressure gauge (Millar Instruments Inc, Houston TX, USA) inserted percutaneously through the femoral artery and advanced into the LV cavity under fluoroscopic guidance [15]. The analogic signals were recorded through an analogic–digital interface (National Instruments), at a sampling rate of 250 Hz [16]. At ten days following thoracic surgery, the hemodynamic parameters were measured during pyruvate injections at rest, during coronary occlusion and at 10′ of coronary reperfusion after the second LAD occlusion. The animals were then sacrificed as described above.

2.6. Statistical analysis

All data were analyzed using MedCalc software (v 12.1, MedCalc Software, Mariakerke, Belgium).

The Kolmogorov–Smirnov test was employed to assess normality of data distribution and for the residuals of regression models. Data are presented as mean ± standard error of the mean (SEM), median and interquartile range (IQR) and as proportions with percentage, as indicated. One-way repeated measures analysis of variance (ANOVA) was used to evaluate whether there was a significant divergence between different measurements. Bonferroni correction for multiple comparison

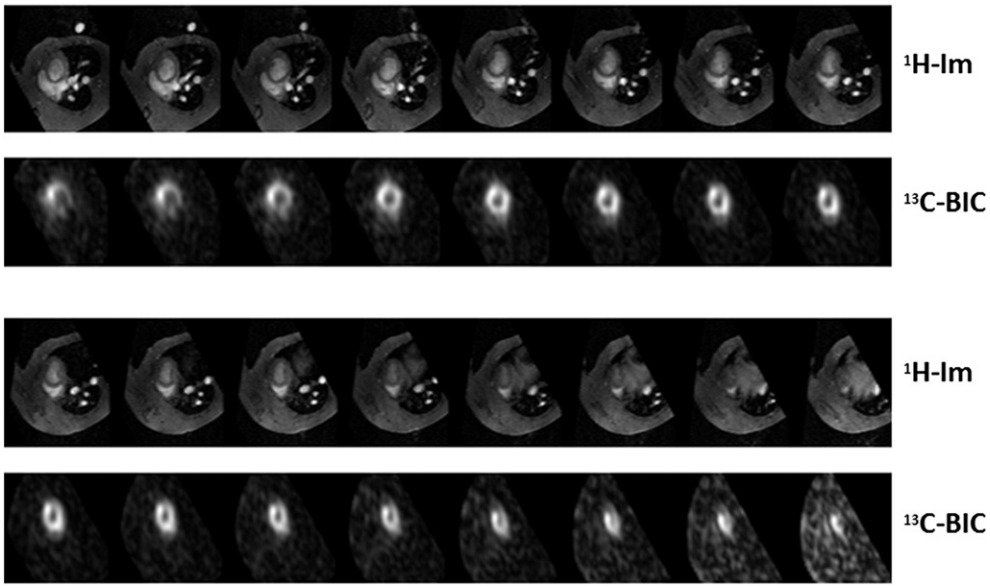

Fig. 2. Reconstructed short axis views of anatomical reference proton images (^{1}H-Im) and metabolic images (^{13}C-bicarbonate images acquired in basal condition, ^{13}C-Bic).

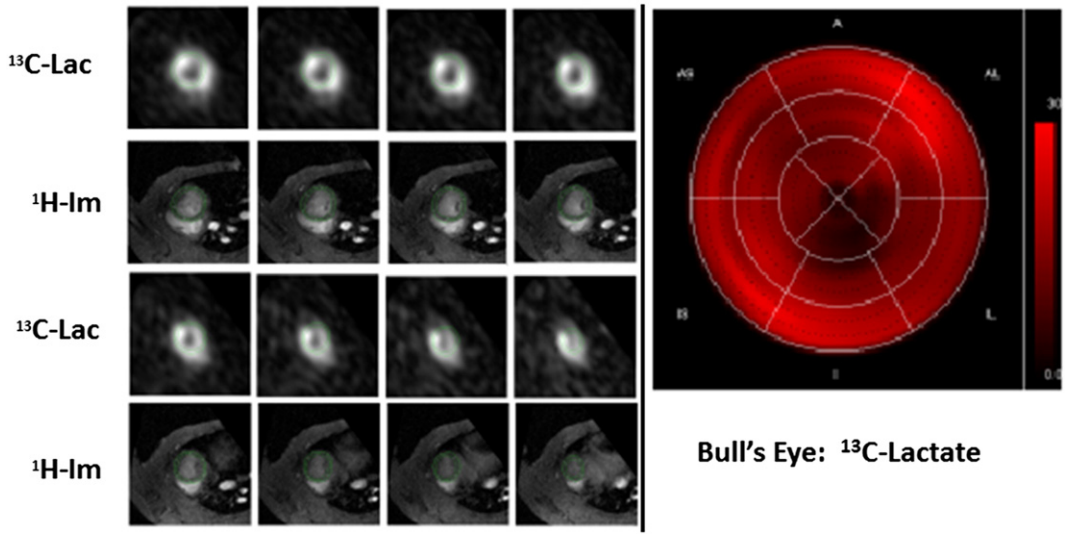

Fig. 3. Illustration of the image analysis procedure: In left panels, short axis view reconstruction of 13C-lactate (13C-Lac) and anatomical proton images (1H-Im); in the anatomical images, the left ventricle was segmented and this segmentation was automatically reproduced in the 13C-lactate maps. Using this segmentation a bull's eye for 13C-lactate was generated (right panel).

was applied. Paired Student's *t*-tests were performed to detect significant differences between groups. In all tests, a two-tailed $p < 0.05$ was considered statistically significant.

3. Results

3.1. Coronary occlusion

Average MAM of lactate and bicarbonate at baseline and during occlusion is shown in Fig. 4. ANOVA analysis revealed a significant dependence of MAM from segmental location in both lactate ($P < 0.001$) and bicarbonate ($P < 0.001$). As shown by the figure, the lactate distribution, the average of metabolic change and the value of MAM detected in the ischemic segments (middle anteroseptal and anterior wall and the apical septum) were significantly different from of the remote regions (inferior and inferolateral segments). As regards bicarbonate distribution ischemic segments were significantly different from the remote segments.

This segmental localization of metabolic changes matched the regional distribution of myocardial segments involved in the ischemic process as evidenced by the histologic evaluation with methylene blue (Fig. 1).

3.2. Reperfusion after ten minutes occlusion

Average MAM from all experiments in segmental distribution of lactate and bicarbonate in either basal or reperfusion condition is shown in Fig. 5. ANOVA analysis revealed significant inhomogeneity of MAM segmental distribution of bicarbonate ($P < 0.001$). No significant difference among segments was found in lactate distribution among segments ($P = 0.302$). As regards bicarbonate distribution ischemic segments were significantly different from the remote.

3.3. Hemodynamics

Heart rate and ECG were not significantly affected by the pyruvate injections: as shown in Table 1, the hemodynamic parameters were unchanged during the pyruvate injection as compared to the corresponding value at each experimental condition (resting, occlusion and reperfusion) before the pyruvate bolus injection.

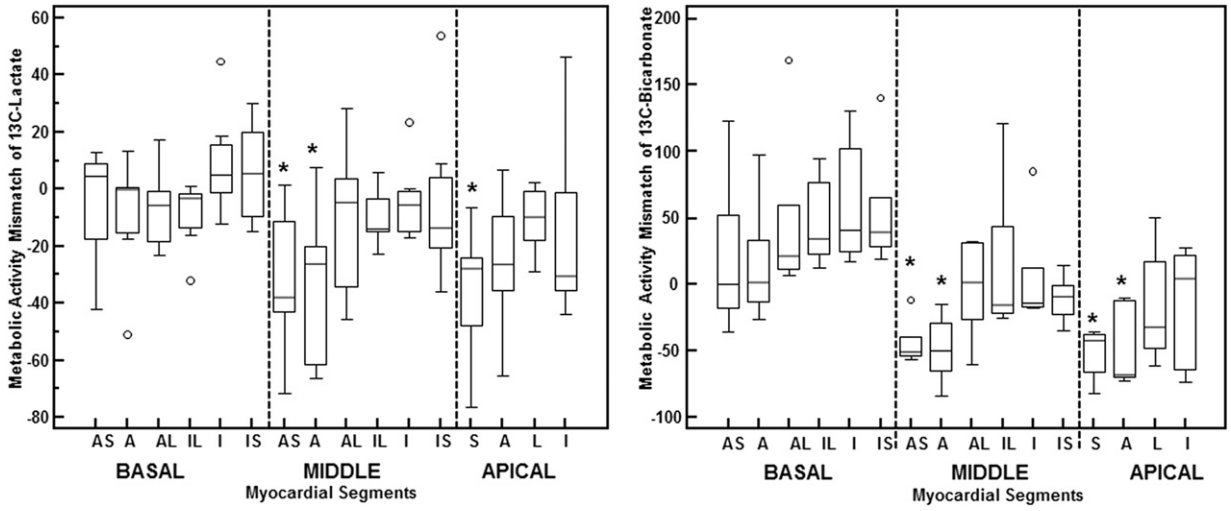

Fig. 4. Metabolic Activity Mismatch (MAM) between basal and during coronary occlusion for 13C-lactate (left) and 13C-bicarbonate (right). AS = anteroseptal; A = anterior; AL = anterolateral; IL = inferolateral; I = inferior; IS = inferoseptal; S = septal.

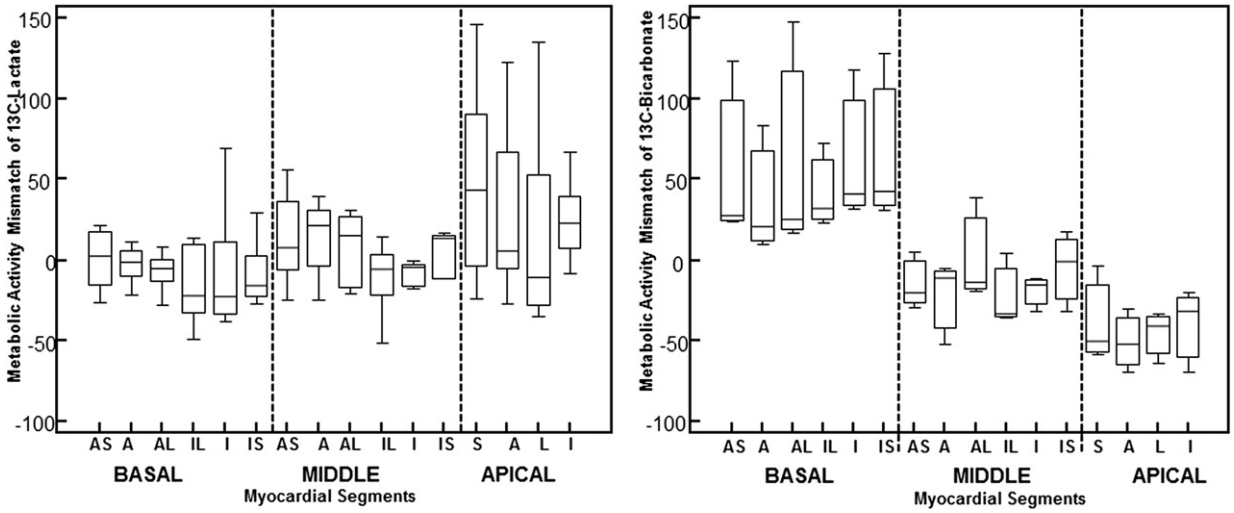

Fig. 5. Metabolic Activity Mismatch (MAM) between basal condition and after reperfusion for 13C-lactate (left) and 13C-bicarbonate (right). AS = anteroseptal; A = anterior; AL = anterolateral; IL = inferolateral; I = inferior; IS = inferoseptal; S = septal.

3.4. Area at risk and metabolic changes

Myocardial regions of LV were divided in the two clusters represented by segments involved by ischemic process at anatomical analysis and remote segment metabolic activity. During occlusion, lactate distribution demonstrated a significantly lower MAM in ischemic segments than in remote segments (-21 ± 6 vs 3 ± 5, $P < 0.001$). Bicarbonate metabolic activity was lower in ischemic than in remote segments (-29 ± 7 vs 33 ± 6, $P < 0.0001$).

Following reperfusion, a significant increase in lactate signal (20 ± 10 vs -7 ± 5, $P = 0.007$) and a significant decrease of bicarbonate signal (-38 ± 12 vs 36 ± 11, $P < 0.0001$) was detected in segments affected by occlusion than in remote segments.

The average extent of region metabolic mismatch during occlusion was 12 ± 5% of LV mass. The extent of area at risk evaluated by methylene blue was 14 ± 7% of LV mass. The mean difference of extent between the area at risk assessed by methylene blue and by hyperpolarized [1-13C]-pyruvate was 5 ± 2%.

3.5. Inter-study reproducibility

The injection of hyperpolarized [1-13C]-pyruvate was repeated during LAD occlusion in 4 pigs. The average variation of the extent of area at risk in the same pigs, measured in different days was 6 ± 2% of LV mass. During reperfusion, we obtained an average variation of 13-lactate extent of 10 ± 4%. This greater difference may be attributed to the changes in haemodynamic parameters in ischemic conditions in different days.

4. Discussion

The present study shows that MRI with hyperpolarized [1-13C]-pyruvate using a 3D-IDEAL Spiral CSI pulse sequences can provide an accurate evaluation of pyruvate, lactate and bicarbonate distribution in either normoperfused or ischemic myocardium, in an animal model mirroring a clinically relevant condition.

In the healthy heart, 60% to 90% energy production is achieved from beta-oxidation of fatty acids, while mainly from pyruvate oxidation for the remainder [17]. Pyruvate is a central metabolic substrate linking glycolysis to the Krebs cycle, and leading to energy production, as well as to production of lactate and CO_2, partly converted in bicarbonate. Pyruvate derives from cytosolic glycolysis and lactate oxidation and, in the normoperfused heart, is mostly oxidized in the Krebs cycle, to form CO_2, and partly either reduced back to lactate or converted into alanine [18].

Magnetic resonance with hyperpolarized 13C-pyruvate allows in-vivo evaluation of relative changes of pyruvate metabolites as lactate, bicarbonate and alanine [3]. Metabolic evaluation may be clinically relevant in ischemic heart disease, as well as in cardiomyopathy.

However, the objective of the current study was to test the sensitivity of the employed methodology in detecting areas of ischemia during coronary occlusion and eventually the subsequent restoration of metabolism during the reperfusion phase. The main finding is the demonstration that spatial resolution obtained using a 3D-IDEAL Spiral CSI pulse sequence was high enough to provide three-dimensional information of acute changes of pyruvate and metabolites in left ventricular myocardium using the conventional on a regional segmentation. Moreover, a

Table 1
Haemodynamic parameters.

	Rest	Rest Pyruvate	Occlusion	Occlusion Pyruvate	Reperfusion	Reperfusion Pyruvate
CBF ml/min	30 ± 3.66	27 ± 3.62	6.1 ± 0.55*	10.2 ± 3*	25.4 ± 2.2	24.3 ± 2.53
CSF nl/beat	0.29 ± 0.04	0.29 ± 0.05	0.07 ± 0.006*	0.09 ± 0.01*	0.29 ± 0.04	0.28 ± 0.02
HeartRate, bpm	100 ± 8.24	96.4 ± 9.8	75.9 ± 7.59*	72.3 ± 7.3*	93.6 ± 18.5	95.4 ± 15.2
SAP, mm Hg	118.17 ± 6.08	113.4 ± 7.99	102.2 ± 13.5	100.5 ± 15.4	124.7 ± 35.3	122.4 ± 30.2
DAP, mm Hg	86.17 ± 4.4	85.7 ± 4.62	69.2 ± 11.5*	66.3 ± 12.4*	86.5 ± 25.1	83 ± 22.5
MAP, mm Hg	104.6 ± 5.16	103.2 ± 5.86	86 ± 12.4*	77.7 ± 11.5*	105.5 ± 29.2	98.5 ± 25.4
LVESP, mm Hg	117.7 ± 6.16	112.87 ± 8.13	100 ± 14	101 ± 12	122 ± 34.6	120 ± 33.4
LVEDP, mm Hg	1.43 ± 0.57	1.95 ± 0.73	1.55 ± 0.5	2.05 ± 0.8	5 ± 3	6.2 ± 2.8
$LVdP/dt_{max}$, mm Hg/s	2468.62 ± 203.1	2238.6 ± 196	1584 ± 225*	1597 ± 213*	2626 ± 1217	2611 ± 1110
$LVdP/dt_{min}$, mm Hg/s	−1704.3 ± 190.7	−1551 ± 218	−1004 ± 318*	−1010 ± 330*	−1245.2 ± 412	−1250 ± 422

Mean values ± SEM; CBF, coronary blood flow; CSF, coronary stroke flow; SAP, systolic arterial pressure; DAP, diastolic arterial pressure; MAP, mean arterial pressure; LVESP, left ventricular end-systolic pressure; LVEDP, left ventricular end-diastolic pressure. *$P < .05$ vs baseline.

good concordance of regional distribution between areas at risk evidenced with methylene blue at histology and the regions with metabolic changes at MRI was found.

During acute coronary occlusion no signal related to pyruvate metabolites was detected in the involved myocardial segments. This was expected, as in such condition the 13C-labeled substrate could not reach the myocardial area at risk because the absence of perfusion prevents the arrival of exogenous pyruvate to the myocardium and, obviously, metabolism of endogenous pyruvate was not evaluable by the present approach.

Myocardial uptake of [1-13C]-pyruvate occurs during the reperfusion phase and changes in metabolites may be detected. In fact, lactate production was slightly increased during reperfusion, while the bicarbonate production was significantly reduced within the area at risk. Based on these results we might speculate that, after 5 min of reperfusion following 10 min of occlusion, the oxidative metabolism was still impaired, showing typical alterations associated with acute ischemia.

MRI with hyperpolarized 13-C technique does not permit a quantitative assessment of metabolites concentration, but only the appreciation of relative changes of pyruvate and its metabolites. In the current study, we evaluated the signal of each myocardial segment in the reconstructed metabolic maps as the difference between the signal of the each segment and the average signal of the entire myocardium, expressed as percentage of the average signal of the entire myocardium. Therefore, the MAM index was used to evaluate the variations of metabolite signal of the same myocardial segment in different conditions (either coronary occlusion or reperfusion versus baseline).

On the technical point of view, in the current study we used the IDEAL spiral CSI method which is different from previously presented approaches. In the study by Golman a single slice 13C chemical shift images in a single short-axis view midway through the long axis of the left ventricle with a slice thickness of 20 mm, and a two-dimensional pixel size of 7.5 × 7.5 mm was used [7]. Lau et al. already described a multislice cardiac-gated spiral 13C imaging pulse sequence consisting of a large permitting whole-heart coverage [8]. However, differently from the above mentioned technique, in the IDEAL spiral CSI method the spectra are not just assumed to be sparse but that the spectral sparsity is used as prior knowledge and then effectively utilized in the reconstruction process, where it allows mapping of the full spectrum rather than a limited number of peaks at certain prescribed frequencies [10]. Thus, the IDEAL spiral CSI pulse sequence permits to get the complete 3D-dataset of information, with optimal signal to noise ratio and with short acquisition time (17 seconds), for each metabolites simultaneously. This might be potentially relevant for the application of hyperpolarized [1-13C]-pyruvate in human allowing complete acquisition during one breath-hold and then permitting to minimize the artifact from respiratory motion.

Recently Schroeder et al. evaluate myocardial metabolism with hyperpolarized [1-13C]-pyruvate in a pig model of pacing induced heart failure using a surface phased array coil [19]. Surface coil allows increase of signal from the cardiac structure next to the coil but produces signal decrease of the distant region as the inferior myocardial segments of LV. In the current study we performed hyperpolarized [1-13C]-pyruvate acquisition using a volumetric bird-cage coil which allowed a more homogeneous signal in all the myocardial sections.

Large dose injection of pyruvate could have a pharmacodynamic effect that should be considered [20]. In this study, heart rate and ECG were not significantly affected by the pyruvate injections (see Table 1). The same findings have been reported by Goldman et al. [9] with a dose of 300 mM of pyruvate. Moreover, a study by Atherton et al. [3] provided the evidence that even after an elevated plasma peak of pyruvate no significant alteration in the concentration of glucose, insulin, lactate, β-idroxybutyrate, triacylglyceride and non esterified fatty acids were detected during the MRS time frame experiments. Moreover, we analyzed in a previous study [4] the cardiac spectroscopic signal after the infusion of 230 mM of hyperpolarized pyruvate at rest and during inotropic stress. We have shown that the cardiac work increased the signal of lactate and bicarbonate, leading to a two-fold increase in the apparent enzymatic kinetic constants in non-steady state conditions. This finding parallels with a two-fold increase in the rate-pressure product stress versus rest, an indirect parameter of cardiac oxygen consumption during inotropic stress, and could partially exclude enzyme saturation effects.

Some limitations of this study should be mentioned: pulse sequence used to acquire images was not ECG-triggered. This approach might have caused motion artifacts and conditioned the spatial resolution; however, the signal was acquired throughout the whole cardiac cycle to increase the SNR, also considering the fast signal decay which is intrinsic to the use of hyperpolarized substrates. In fact, the signal of magnetization undergoes an exponential decay with typical time constants (T1, spin lattice relaxation time) of about 60 s.

For these reasons, at present, we were forced to use the whole allowed time to get enough signal from the myocardium.

Another limitation was that only changes in bicarbonate and lactate were assessed, while alanine changes were not systematically detected. In fact, the alanine signal resulted rather low and in some segments was not detectable, due to a low signal to noise ratio. This limitation was the consequence of evaluation of cardiac metabolism using a whole-heart three dimensional approach and using a birdcage volumetric coil.

Further studies are needed to verify if these limitations can be overcome, using a surface coil to improve the SNR, as well as an accurate ECG triggering might allow a better identification of regional metabolic changes.

5. Conclusions

This study shows that a three-dimensional evaluation of cardiac metabolism with 13C hyperpolarized pyruvate is feasible in a large size animal model of ischemia and reperfusion. A good topographic correlation on segmental basis was found between spectroscopic imaging maps and gross anatomical analysis. The Food and Drug Administration recently approved the use of hyperpolarized 13C-pyruvate for clinical studies of prostate cancer. Previous studies and the present one point to the possibility that, in the near future, H13C-tracing may be used as a powerful diagnostic tool in the cardiovascular field.

Conflict of interest

The authors report no relationships that could be construed as a conflict of interest.

Acknowledgment

None.

References

[1] Månsson S, Johansson E, Magnusson P, Chai CM, Hansson G, Petersson JS, et al. 13C imaging—a new diagnostic platform. Eur Radiol 2006;16:57–67.
[2] Schroeder M, Cochlin L, Heather L, Clarke K, Radda G, Tyler D. In vivo assessment of pyruvate dehydrogenase flux in the heart using hyperpolarized carbon-13 magnetic resonance. Proc Natl Acad Sci U S A 2008;105:12051–6.
[3] Atherton HJ, Schroeder MA, Dodd MS, Heather L, Carter E, Cochlin LE, et al. Validation of the in vivo assessment of pyruvate dehydrogenase activity using hyperpolarised 13C-magnetic resonance spectroscopy. NMR Biomed 2011;24:201–8.
[4] Menichetti L, Frijia F, Flori A, Wiesinger F, Lionetti V, Giovannetti G, et al. Assessment of real-time myocardial uptake and enzymatic conversion of hyperpolarized [1-13C]pyruvate in pigs using slice selective magnetic resonance spectroscopy. Contrast Media Mol Imaging 2012;7:85–94.
[5] Schroeder MA, Clarke K, Neubauer S, Tyler DJ. Hyperpolarized magnetic resonance: a novel technique for the in vivo assessment of cardiovascular disease circulation. 2011;124:1580–94.
[6] Schroeder MA, Atherton HJ, Ball D, Heather LC, Cole M, Griffin J, et al. Real time assessment of Krebs cycle metabolism using hyperpolarized 13C magnetic resonance spectroscopy. FASEB J 2009;23:2529–38.

[7] Golman K, Petersson JS, Magnusson P, Johansson E, Akeson P, Chai CM, et al. Cardiac metabolism measured noninvasively by hyperpolarized 13C MRI. Magn Reson Med 2008;59:1005–13.
[8] Lau AZ, Chen AP, Ghugre NR, Ramanan V, Lam WW, Connelly KA, et al. Rapid multislice imaging of hyperpolarized (13)C pyruvate and bicarbonate in the heart. Magn Reson Med 2010;64:1323–31.
[9] Reeder SB, Pineda AR, Wen Z, Shimakawa A, Yu H, Brittain JH, et al. Iterative decomposition of water and fat with echo asymmetry and least-squares estimation (IDEAL): application with fast spin-echo imaging. Magn Reson Med 2005;54:636–44.
[10] Wiesinger F, Weidl E, Menzel MI, Janich MA, Khegai O, Glaser SJ, et al. IDEAL spiral CSI for dynamic metabolic MR imaging of hyperpolarized [1-(13) C]pyruvate. Magn Reson Med 2011. http://dx.doi.org/10.1002/mrm.23212 [Epub ahead of print].
[11] Martorana PA, Göbel H, Kettenbach B, Nitz RE. Comparison of various methods for assessing infarct-size in the dog. Basic Res Cardiol 1982;77:301–8.
[12] Ardenkjaer-Larsen JH, Fridlund B, Gram A, Hansson G, Hansson L, Lerche MH, et al. Increase in signal-tonoise ratio of >10,000 times in liquidstate NMR". Proc Natl Acad Sci U S A 2003;100:10158–63.
[13] Cerqueira MD, Weissman NJ, Dilsizian V, Jacobs AK, Kaul S, Laskey WK, et al. Standardized myocardial segmentation and nomenclature for tomographic imaging of the heart: a statement for healthcare professionals from the Cardiac Imaging Committee of the Council on Clinical Cardiology of the American Heart Association. Circulation 2002;105:539–42.
[14] Jageneau AH, Schaper WK, Van Gerven W. Enhancement of coronary reactive hyperemia in unanesthetized pigs by an adenosine-potentiator (Lidoflazine). Naunyn Schmiedebergs Arch Pharmakol 1969;265(1):16–23.
[15] Simioniuc A, Campan M, Lionetti V, Marinelli M, Aquaro GD, Cavallini C, et al. Placental stem cells pre-treated with a hyaluronan mixed ester of butyric and retinoic acid to cure infarcted pig hearts: a multimodal study. Cardiovasc Res 2011;90:546–56.
[16] Lionetti V, Guiducci L, Simioniuc A, Aquaro GD, Simi C, De Marchi D, et al. Mismatch between uniform increase in cardiac glucose uptake and regional contractile dysfunction in pacing-induced heart failure. Am J Physiol Heart Circ Physiol 2007;293:H2747–56.
[17] Stanley WC, Recchia FA, Lopaschuk GD. Myocardial substrate metabolism in the normal and failing heart. Physiol Rev 2005;85:1093–129.
[18] Randle PJ. Fuel selection in animals. Biochem Soc Trans 1986;14:799–806.
[19] Schroeder MA, Lau AZ, Chen AP, Gu Y, Nagendran J, Barry J, et al. Hyperpolarized (13)C magnetic resonance reveals early- and late-onset changes to in vivo pyruvate metabolism in the failing heart. Eur J Heart Fail 2013;15:130–40.
[20] Moreno KC, Sabelhaus SM, Merritt ME, Sherry AD, Malloy CR. Competition of pyruvate with physiological substrates for oxidation by the heart: implications for studies with hyperpolarized [1-13C]pyruvate. Am J Physiol Heart Circ Physiol 2010;298:H1556–64.